Brefeldin A-dependent Membrane Tubule Formation Reconstituted In Vitro Is Driven by a Cell Cycle–regulated Microtubule Motor

Alasdair M. Robertson and Victoria J. Allan*

School of Biological Sciences, University of Manchester, Manchester M13 9PT, United Kingdom

Treatment of cultured cells with brefeldin A (BFA) induces the formation of extensive membrane tubules from the Golgi apparatus, *trans*-Golgi network, and early endosomes in a microtubule-dependent manner. We have reconstituted this transport process in vitro using *Xenopus* egg cytosol and a rat liver Golgi-enriched membrane fraction. The presence of BFA results in the formation of an intricate, interconnected tubular membrane network, a process that, as in vivo, is inhibited by nocodazole, the H1 anti-kinesin monoclonal antibody, and by membrane pretreatment with guanosine 5′-*O*-(3-thiotriphosphate). Surprisingly, membrane tubule formation is not due to the action of conventional kinesin or any of the other motors implicated in Golgi membrane dynamics. Two candidate motors of ~100 and ~130 kDa have been identified using the H1 antibody, both of which exhibit motor properties in a biochemical assay. Finally, BFA-induced membrane tubule formation does not occur in metaphase cytosol, and because membrane binding of both candidate motors is not altered after incubation in metaphase compared with interphase cytosol, these results suggest that either the ATPase or microtubule-binding activity of the relevant motor is cell cycle regulated.

INTRODUCTION

Microtubules, and their associated motor proteins, play a central role in maintaining the spatial organization of the secretory and endocytic pathways (reviewed in Lane and Allan, 1998). Furthermore, microtubule motors are involved not only in the maintenance of organelle structure but also in facilitating the tubovesicular transport of membrane and protein between organelles. Some of these transport steps are conveniently emphasized by treating cultured cells with the fungal metabolite brefeldin A (BFA). Under these conditions the Golgi apparatus very quickly forms membrane tubules, which move along microtubules and fuse with the endoplasmic reticulum (ER), resulting in a dramatic redistribution of Golgi apparatus components into the ER and the loss of the Golgi apparatus as a discrete organelle (Lippincott-Schwartz et al., 1990), and it has been suggested that this represents an enhanced version of the normal Golgi-to-ER

transport process (Klausner et al., 1992; Lippincott-Schwartz, 1993). The formation of BFA-induced Golgi tubules has been shown to be dependent on microtubule motor activity, because it is inhibited by the microinjection of the H1 monoclonal antibody (Lippincott-Schwartz et al., 1995), which was raised against the plus end–directed motor kinesin from bovine brain (Bloom et al., 1988; Hirokawa et al., 1989; Elluru et al., 1995).

BFA also causes microtubule-dependent tubule extension and redistribution of both the *trans*-Golgi network (TGN) and early endosomes (Lippincott-Schwartz et al., 1991; Wood et al., 1991; Reaves and Banting, 1992). The TGN tubules do not appear to fuse with the ER but instead fuse with the early endosomal network. The suppression of conventional/ubiquitous kinesin heavy chain (uKHC) expression using an antisense approach inhibited the formation of tubules containing either mannose-6-phosphate receptor (an endosomal and TGN marker) or the fluid phase endocytic marker lucifer yellow, suggesting that uKHC may be the motor that drives the outward movement of TGN and endosomal BFA tubules (Feiguin et al., 1994). Interestingly, the same treatment did not inhibit the BFA-induced redistribution of Golgi enzymes into the ER (Feiguin et al., 1994), in seeming contradiction to the results of Lippincott-Schwartz et al. (1995).

To study the properties of the motor proteins involved in BFA-induced membrane tubule formation more closely, we

---

* Corresponding author. Email address: viki.allan@man.ac.uk.
Abbreviations used: AMP.PNP, 5′-adenylyl imidodiphosphate; BFA, brefeldin A; COP, coatomer protein; ER, endoplasmic reticulum; GTPγS, guanosine 5′-*O*-(3-thiotriphosphate); IgG, immunoglobulin G; KHC, kinesin heavy chain; KLP, kinesin-like protein; nKHC, neuronal KHC, mAb, monoclonal antibody; RT, room temperature; TGN, *trans*-Golgi network; uKHC, ubitquitous KHC; VE-DIC, video-enhanced differential interference contrast microscopy.

have developed an in vitro assay combining a rat liver Golgi-enriched membrane preparation with *Xenopus* egg cytosol. Such cytosols are ideal for studying microtubule-driven membrane movement, because they polymerise microtubules and support membrane motility at room temperature, and furthermore, the cell cycle state of these extracts is relatively easy to manipulate (Allan, 1993). It has previously been shown that interphase cytosols support the microtubule-dependent formation of *Xenopus*-derived ER networks and the movement of small vesicles, whereas metaphase cytosols do not (Allan and Vale, 1991; reviewed in Robertson and Allan, 1997). In metaphase, cytoplasmic dynein-driven membrane movement is thought to be inactivated by the phosphorylation of cytoplasmic dynein light intermediate chains, which correlates with detachment of cytoplasmic dynein from the membrane (Niclas *et al.*, 1996). In addition, interphase, but not metaphase, cytosol has been shown to support the movement of membranes purified from rat liver (Allan and Vale, 1991, 1994). Because membrane traffic is generally inhibited as cells enter mitosis (reviewed in Warren, 1985), it would be of interest to determine whether the effect of BFA on membrane dynamics is also cell cycle regulated.

In this study we have reconstituted BFA-induced membrane tubule formation in vitro. This tubule extension is driven by microtubule motor activity and is inhibited by the H1 monoclonal anti-kinesin antibody. Surprisingly, this movement was not generated by the action of conventional kinesin. Instead, H1 recognized two proteins that behaved like kinesin-like proteins (KLPs) but were distinct from conventional kinesin or any of the other motor proteins currently implicated in Golgi membrane dynamics. Finally, BFA-induced membrane tubule formation does not occur in metaphase cytosol, demonstrating that the motor involved is cell cycle regulated.

MATERIALS AND METHODS

Materials

Antibodies and other reagents were generously provided by the following people: H1 monoclonal antibody (mAb) (Pfister *et al.*, 1989) from Dr. G. Bloom (University of Texas Southwestern Medical Center, Dallas, TX); SUK 4 hybridoma (Ingold *et al.*, 1988) from Dr. J. Scholey (University of California, Davis, CA); rabbit anti-Rabkinesin 6 (Echard *et al.*, 1998) from Dr. B. Goud (Institut Curie, Paris, France); rabbit anti-KIF1C (Dorner *et al.*, 1998) from Dr. R. Lammers (Max-Planck Institut für Biochemie, Martinsried, Germany); rabbit anti-uKHC, affinity-purified rabbit anti-neuronal kinesin heavy chain (nKHC) (Niclas *et al.*, 1994), and bovine brain tubulin from Dr. R. Vale (University of California, San Francisco, CA); bacterially expressed rat kinesin heavy chain head domain from Dr. R. Cross (Marie Curie Research Institute, Oxted, Surrey, United Kingdom); rabbit anti-HIPYR and anti-LAGSE (originally raised by Dr. T. Mitchison and coworkers; Sawin *et al.*, 1992) and monoclonal anti-kinesin II (85-kDa subunit: originally raised by Dr. J. Scholey; Cole *et al.*, 1993) from Dr. V. Gelfand (University of Illinois, Urbana, IL); maD, which recognizes β-coatomer protein (β-COP) (Pepperkok *et al.*, 1993), from Dr. T. Kreis, (University of Geneva, Geneva, Switzerland); rabbit anti-GM130 (Nakamura *et al.*, 1995) and anti-giantin from Dr. G. Warren (Imperial Cancer Research Fund, London, United Kingdom); rabbit anti-TGN38 (Luzio *et al.*, 1990) from Dr. P. Luzio (University of Cambridge, Cambridge, United Kingdom); and 1D3, which recognizes a KDEL-containing peptide (Vaux *et al.*, 1990), from Dr. D. Vaux (University of Oxford, Oxford, United

Kingdom). Monoclonal H68.4 against human transferrin receptor was obtained from Zymed (San Francisco, CA), and sheep anti-rat albumin was from Cappel/Organon Teknika (Turnhout, Belgium). BFA and Taxol (paclitaxel) were purchased from LC Laboratories (Nottingham, United Kingdom). Sucrose (ultrapure grade) was purchased from Life Technologies (Paisley, United Kingdom). Unless otherwise stated, all other reagents were purchased from Sigma (Poole, Dorset, United Kingdom) or BDH (Poole, Dorset, United Kingdom).

Preparation of Xenopus Egg Cytosols and the Rat Liver Golgi Membrane Fraction

Concentrated interphase- and metaphase-arrested *Xenopus* egg extracts were prepared and analyzed for cell cycle status as described previously (Allan and Vale, 1991; Allan, 1993, 1998; Lane and Allan, 1999). High-speed cytosols were then prepared by diluting the extracts with 2 vol of acetate buffer (100 mM K-acetate, 3 mM Mg-acetate, 5 mM EGTA, 10 mM HEPES, pH 7.4) containing 150 mM sucrose, 7.5 mM creatine phosphate, and 1 mM MgATP, and then spinning at 55,000 rpm ($117,000 \times g_{av}$), for 30 min at 4°C, in a TLA100 rotor (Beckman, High Wycombe, Bucks, United Kingdom). These cytosolic fractions were used to study BFA-induced membrane tubule movement (see RESULTS). To compare this novel motility with the previously observed "ball-domain" tubule motility (Allan and Vale, 1994), high-speed supernatants were also prepared from extracts made by crushing dejellied eggs in 1.5 vol of acetate buffer (for details, see Allan and Vale, 1994).

A Golgi-enriched membrane fraction (protein concentration ~4.0 mg/ml) was prepared from rat liver (Leelavathi *et al.*, 1970), with the modifications described (Allan and Vale, 1991). More concentrated Golgi membranes (~10 mg/ml) were obtained by collecting only the largest membrane aggregates.

Motility Assays and Microscopy

Motility assays were generally performed as described (Allan and Vale, 1994; Allan, 1998) using 8 μl of *Xenopus* egg cytosol plus 1 μl of rat liver Golgi membrane fraction, 0.5 μl of BFA (2 mg/ml), and 0.5 μl of acetate buffer. The 0.5 μl of acetate buffer was substituted with nocodazole (to 4 μM), guanosine 5'-O-(3-thiotriphosphate) (GTPγS; to 0.25 mM), or sodium orthovanadate (to 40 μM). BFA stock solutions (10 mg/ml in methanol) were stored at −20°C and diluted to 2 mg/ml in acetate buffer immediately before use. The direction of vesicle movement was assayed using demembranated, salt-washed axoneme fragments from *Tetrahymena* (Allan and Vale, 1991). Motility was followed by video-enhanced differential interference contrast microscopy (VE-DIC) in real time using an Olympus Optical (Tokyo, Japan) BX60 microscope equipped with DIC optics (Allan, 1998). The RETRAC object tracking system (Dr. N. Carter, Marie Curie Research Institute, Oxted, Surrey, United Kingdom) was used to determine rates of movement from videotape sequences and to digitize single frames. To analyze the extent of membrane tubule formation under each incubation condition, the membrane networks were traced directly onto acetate sheets, and tubule length was determined using a map measuring tool.

Antibody inhibition studies were carried out as follows: rat liver Golgi membranes were preincubated on ice with either the H1 ascites or a control c-*myc* ascites for 25 min at a 5:1 ratio. Alternatively, Golgi membranes were preincubated on ice with either the SUK 4 monoclonal antibody (Ingold *et al.*, 1988; ~5 mg/ml in PBS [140 mM NaCl, 2.7 mM KCl, 1.5 mM KH₂PO₄, 8.1 mM Na₂HPO₄]) or a control purified mouse immunoglobulin G (IgG; 5 mg/ml in PBS) for 45 min at a 4:1 ratio. The membranes were then used in motility assays as described above. The presence of ascites often reduced microtubule polymerization (for unknown reasons), which was countered by pretreating the perfusion chambers with cytosol (diluted 1:5 with acetate buffer) containing 100 μg/ml BFA for 5 min. When analyzing the effect of GTPγS on motility, 0.25 mM

GTPγS was added to rat liver Golgi membranes in interphase cytosol for 5 min at room temperature (RT) and then 10 min on ice, followed by the addition of 100 μg/ml BFA, or membranes and cytosol were incubated with BFA for 5 min at RT and then 10 min on ice before the addition of GTPγS.

Immunofluorescence analysis of the BFA-induced membrane networks and ball-domain networks assembled for 40–45 min was performed as described (Allan and Vale, 1994) except that 0.5% (wt/vol) tannic acid in acetate sucrose buffer was flowed through the chamber to stabilize the membrane tubules, instead of flowing through buffer containing fixative. The coverslips were then fixed in methanol and processed for immunofluorescence (Allan and Vale, 1994). Primary antibody dilutions are as follows: anti-giantin, 1:500; anti-albumin, 1:1000; anti-transferrin receptor, 1:100; and anti-TGN38, 1:400. Alexa 488- and Alexa 594-conjugated (Molecular Probes, Leiden, The Netherlands) and Texas Red-conjugated (Jackson ImmunoResearch, West Grove, PA) secondary antibodies were used at 1:200 or 1:400. Images were obtained using an Olympus BX-60 microscope with a UplanFl 100 × 1.30 numerical aperture Pol objective and appropriate filter sets, coupled to a MicroMax slow-scan, cooled charge-coupled device camera (Roper Scientific, Marlow, Bucks, United Kingdom) driven by MetaMorph software (Universal Imaging, West Chester, PA).

Microtubule Binding and ATP Release of Motor Proteins

Microtubules were polymerized from purified bovine brain tubulin as described (Vale and Toyoshima, 1988), stabilized with 20 μM Taxol, and stored at −80°C. For each microtubule binding/ATP release assay, rat liver Golgi membranes (125 μl) were made up to 10 U/ml hexokinase, 20 μM glucose, 20 μM Taxol, 400 μM 5′-adenylyl imidodiphosphate (AMP.PNP), 0.5% Triton TX-100 (Surfact-Amps X-100; Pierce, Chester, United Kingdom), 1 mM DTT, 10 μg/ml protease inhibitors (leupeptin, chymostatin, pepstatin, and aprotinin), and 1 μg/ml cytochalasin D, and were incubated for 5 min at RT. Finally, Taxol-stabilized microtubules were added to 0.13 mg/ml, and the mixture was incubated at RT for 30 min. The mixture was then layered onto a cushion of 40% sucrose in BRB80 (80 mM 1,4-piperazinediethanesulfonic acid, 2 mM MgCl$_2$, 1 mM EGTA, pH 7.4 with KOH) containing 1 mM DTT, 1 μg/ml cytochalasin D, 2.5 μg/ml protease inhibitors, and 4 μM Taxol, and the microtubules were recovered by spinning at $68,000 \times g_{av}$ for 20 min at 22°C in a TLS55 rotor (Beckman). The proteins in the supernatant and cushion were recovered by chloroform/methanol precipitation (Wessel and Flugge, 1984) and prepared for SDS-PAGE and immunoblotting. The microtubule pellets were resuspended in 12.5 μl of BRB80 containing 5 mM MgATP, 1 mM DTT, 10 μg/ml protease inhibitors, and 10 μg/ml cytochalasin D and were incubated at RT for 25 min. Microtubules were then separated from the ATP release supernatant by spinning for 15 min at $68,000 \times g_{av}$ in the TLS55 rotor. The entire microtubule pellet fraction was loaded into a single SDS-PAGE gel lane, as were all other fractions. Essentially the same protocol was followed for microtubule binding/ATP release studies carried out under high-salt conditions, except that KCl was substituted with 0.5 M NaCl, and as a control, ATP was substituted with 5 mM AMP.PNP.

When a more concentrated preparation of microtubule motors was required, 300 μl of concentrated rat liver Golgi membranes (protein concentration ~10 mg/ml) were solubilized and incubated under the motor binding conditions detailed above, but with microtubules added to 0.6 mg/ml rather than 0.13 mg/ml.

Immunoprecipitation of uKHC from Golgi Membrane Fractions

Two batches of Protein G beads (Zymed; 100-μl slurry per tube) were blocked by incubation in 20% BSA in PBS for 30 min at 4°C, with constant rotation. One set of beads was incubated with 126 μg of SUK 4, the other with purified mouse IgG, overnight at 4°C with constant rotation. Beads were then washed with PBS and resuspended in 400 μl of rat liver Golgi membranes, which had been solubilized with 1% Triton X-100, and incubated for 2 h on ice, with occasional agitation. The beads were washed four times with PBS and resupended in 2× Laemmli sample buffer.

Analysis of β-COP Membrane Binding after BFA and GTPγS Treatment

Rat liver Golgi membranes (20 μl) were incubated with 112.5 μl of interphase cytosol plus one of the following: 1) 1.5 μl of methanol and 6 μl of acetate buffer; 2) 1.5 μl of BFA (from the 10 mg/ml methanol stock) and 6 μl of acetate buffer; 3) 6.0 μl of GTPγS (to 0.25 mM) for 5 min and then 1.5 μl of BFA; and 4) 1.5 μl of BFA for 5 min and then 6 μl of GTPγS (to 0.25 mM). Samples were incubated at RT for 30 min, then on ice for 15 min, and were then diluted with 200 μl of acetate buffer (containing 1 mM DTT and 1 μg/ml protease inhibitors). Membranes were recovered by spinning at $100,000 \times g_{av}$ in a TLS55 rotor, through a cushion of 400 mM sucrose in acetate buffer, at 4°C.

Analysis of Motor and Membrane Binding in Interphase and Metaphase Cytosols

Thirty microliters of rat liver Golgi membranes were incubated in 120 μl of acetate buffer or in interphase or metaphase cytosol (prepared using 2 vol of acetate buffer without sucrose) for 45 min at RT, followed by 15 min on ice to depolymerise microtubules. Each mixture was then diluted with 500 μl of acetate buffer (containing 1 mM DTT and 1 μg/ml protease inhibitors) and layered onto a 400 mM sucrose/acetate buffer cushion (containing 1 mM DTT and 1 μg/ml protease inhibitors). Membranes were recovered by spinning at $100,000 \times g_{av}$ in a TLS55 rotor for 30 min at 4°C.

PAGE and Immunoblotting

Electrophoresis and immunoblotting were performed as described (Lane and Allan, 1999). Primary antibody dilutions used were: H1 mAb, 1:500; MaD anti-β-COP, 1:2000; rabbit anti-uKHC, 1:4000; affinity-purified rabbit anti-nKHC, 1:300; rabbit anti-HIPYR, anti-LAGSE, anti-Rabkinesin 6, and anti-KIF1C, 1:500; and rabbit anti-GM130, 1:3000. After incubation with horseradish peroxidase-conjugated (Pierce) or alkaline phosphatase-conjugated (Jackson ImmunoResearch) secondary antibodies, blots were developed using the ECL SuperSignal detection kit (Pierce) and exposed to Eastman Kodak (Rochester, NY) X-OMAT LS film or using an alkaline phosphatase nitro blue tetrazolium/5-bromo-4-chloro-3-indolyl phosphate color reaction. Blots were scanned into Adobe (Mountain View, CA) Photoshop using a Sharp (Mahwah, NJ) JX-330 scanner. The public domain NIH image program (developed at the US National Institutes of Health and available on the internet at http://rsb.info.nih.gov/nih-image/) was used for analysis of band intensity on an Apple (Cupertino, CA) Macintosh Power PC.

RESULTS

BFA-induced Membrane Tubule Formation Reconstituted In Vitro Is a Plus End–directed Microtubule Motor-dependent Process

The assay system used in these studies uses a combination of *Xenopus* egg cytosol and a rat liver Golgi membrane fraction that contains stacked and single cisternae, together with large vesicles containing very-low-density lipoprotein particles (Allan and Vale, 1991, 1994). When these membranes were incubated in interphase high-speed supernatant, without BFA, we observed two classes of structures. The first
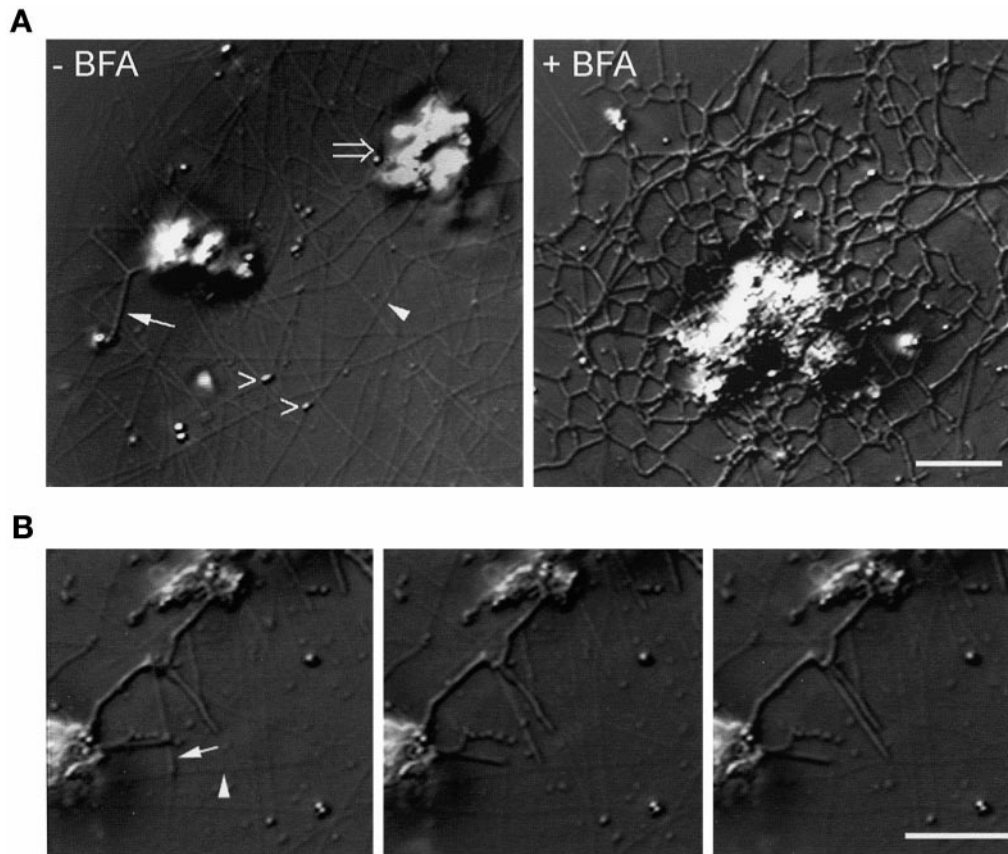
Figure 1. Formation of tubular membrane networks in response to BFA treatment. Rat liver Golgi fraction membranes were incubated in interphase *Xenopus* egg cytosol in the presence and absence of BFA and were observed by VE-DIC. (A) Left panel, typical VE-DIC image of rat liver Golgi membranes incubated in interphase cytosol for 60 min, in the absence of BFA. Microtubules (closed arrowhead) polymerize from endogenous *Xenopus* tubulin, and membrane vesicles (open arrowheads) are observed moving along them. Large membrane clumps (open arrow) are essentially nonmotile, although membrane tubules are occasionally seen extending from them (closed arrow). In the presence of 100 μg/ml BFA (right panel), an intricate and extended tubular membrane network forms. Bar, 5 μm (applies to both panels). (B) Microtubule motor activity of BFA-induced membrane tubules. A sequence of VE-DIC images taken at 5 s intervals shows a typical BFA-induced membrane tubule (arrow) moving along a microtubule (arrowhead). Note that the moving membrane tubule tip does not possess the characteristic globular domain seen in previous studies using different cytosol (Allan and Vale, 1994). Bar, 5 μm (applies to all three panels).

type consisted of a population of highly motile vesicles (Figure 1A, left panel, open arrowheads), which moved toward microtubule plus ends at 1.24 ± 0.03 μm/s (n = 21; Table 1). Vesicle movement remained exclusively plus end directed in the presence of BFA but occurred at a slightly slower rate (1.00 ± 0.04 μm/s; n = 20; Table 1) than in the absence of the drug. The second population of membranes consisted of large, nonmotile clumps (Figure 1A, left panel, open arrow), which only occasionally formed membrane tubules (Figure 1A, left panel, closed arrow). However, when 100 μg/ml BFA was included in the assay, membrane tubules extended out from these clumps within 5 min, and by 30–60 min an intricate tubular membrane network resulted (Figure 1A, right panel, and Table 2). The maximal amount of membrane tubule formation was seen at 100 μg/ml BFA, although a significant amount was observed at concentrations as low as 5 μg/ml (Robertson and Allan, unpublished data).

The membrane network extension was dependent on the presence of microtubules (Table 2), and careful observation of 196 membrane tubule movements revealed that all were driven by membrane-associated motor protein activity and not by static membrane attachment (via tip attachment complexes) to growing or gliding microtubules (Vale and Hotani, 1988; Waterman-Storer *et al.*, 1995). The membrane tubules translocated along microtubules at a rate of 0.25 ± 0.06 μm/s (n = 20) and were determined to be exclusively plus end directed (n = 65; Table 1) by comparison with the direction of vesicle movement movement (known to be 100% plus end directed; Table 1) along the same microtubule.

Because BFA induces tubule formation from the Golgi apparatus, TGN and early endosomes (Lippincott-Schwartz *et al.*, 1989, 1990, 1991; Wood *et al.*, 1991; Sciaky *et al.*, 1997), and in some cases late endosomes and lysosomes (Lippincott-Schwartz *et al.*, 1991), we used an immunofluorescence

Table 1. Analysis of membrane motor properties

	Rate of movement (μm/s)[a]	% plus end	% minus end
Vesicles (no BFA)[b]	1.24 ± 0.03 (n = 21)	100 (n = 35)	0 (n = 35)
Vesicles (+ BFA)[b]	1.00 ± 0.04 (n = 20)	100 (n = 26)	0 (n = 26)
BFA-induced membrane tubules[c]	0.25 ± 0.06 (n = 20)	100 (n = 65)	0 (n = 65)

[a] Rates of movement were measured from videotape using the RETRAC rate analysis function (see MATERIALS AND METHODS).

[b] Direction of vesicle movement was assayed using demembranated, salt-washed axoneme fragments from *Tetrahymena* (see MATERIALS AND METHODS).

[c] The direction of BFA-induced membrane tubule movement was determined by comparing the direction of vesicle movement along a microtubule with the direction of membrane tubule movement along the same microtubule (see MATERIALS AND METHODS).

approach (Allan and Vale, 1994, modified as described in MATERIALS AND METHODS) to identify the membrane networks formed in vitro from the rat liver Golgi fraction. The membrane tubules contained the secretory protein albumin (Figure 2A), as well as the Golgi resident protein giantin (Linstedt and Hauri, 1993). Surprisingly, the networks also labeled with antibodies to TGN38 (Figure 2C′) and to the early endosomal marker transferrin receptor (Figure 2C), both of which colocalized almost completely with giantin (Figure 2B′; Allan, unpublished data) and with each other (Figure 2, C and C′). These results suggest that BFA has induced fusion between elements of the Golgi apparatus, TGN, and early endosomes (see DISCUSSION). However, lysosomes remained as distinct, single organelles (Allan, unpublished data), which demonstrates that indiscriminate fusion is not occurring.

A key questions raised by these results is how these BFA-induced networks relate to the membrane networks we have previously observed forming in the absence of BFA from the same rat liver Golgi membrane fraction when incubated in *Xenopus* egg cytosol prepared using a different protocol (Allan and Vale, 1991, 1994). These latter membrane tubules had a characteristic morphology, with ~90% of moving tubule tips possessing a distinct globular domain (Allan and Vale, 1994), whereas only 11% (n = 90) of the moving tips of BFA-induced membrane tubules described here had a similar "ball-like" structure, with 89% being smooth at their tips (Figure 1B). Moreover, the rate of BFA-induced tubule formation reported here (Table 1) is approximately four times slower than that of the ball-domain tubules, which translocate at 1.13 ± 0.1 μm/s (n = 20).

However, the clearest evidence for the two types of networks being absolutely distinct has been obtained using our improved immunofluorescence method. Although the ball-domain tubules contain albumin (Figure 2D), just like the BFA networks (Figure 2A), the ball-domain tubules do not contain detectable giantin (Figure 2D′), transferrin receptor, or TGN38 (Allan, unpublished data). In addition, because the ball-domain tubules label with an accepted ER marker (1D3, which was raised against a KDEL-containing peptide; Vaux *et al.*, 1990; Figure 2E), these tubules may be formed from smooth ER membranes that are present in the rat liver Golgi fraction or, alternatively, may be derived from intermediate compartment membranes, which would be expected to contain recycling ER markers.

Taken together, these data provide strong evidence that the two networks are functionally and morphologically distinct. It is currently unclear why cytosols prepared using different protocols should promote such distinct types of membrane tubule movement.

The BFA Effect Is Inhibited by the Preaddition of GTPγS

Because the in vitro assay was reconstituting at least one of BFA's in vivo effects, the formation of membrane tubules, we next wanted to determine whether BFA was also disrupting the function of coatomer proteins in vitro. BFA prevents the activation of ADP ribosylation factor 1, which is a small GTP-dependent protein required for membrane traffic through the Golgi apparatus (Donaldson *et al.*, 1992;

Table 2. Membrane tubule extension in the presence of BFA is microtubule dependent

	Experiment 1		Experiment 2	
	(μm of membrane tubule/field)		(μm of membrane tubule/field)	
	−BFA	+BFA	+BFA − nocodazole	+BFA + 4 μM nocodazole
10 min	0.47±0.27	26.4 ± 3.1	25.8 ± 3.16	0.59 ± 0.3
60 min	4.7±1.15	90.9 ± 8.7	77.8 ± 7.9	2.37 ± 0.89

The length of membrane tubules present per field (micrometers) was determined for 25 fields after a 10- and 60-min incubation, and the average values are expressed ± SEM.

Brefeldin A-induced tubules

"Ball-domain" tubules
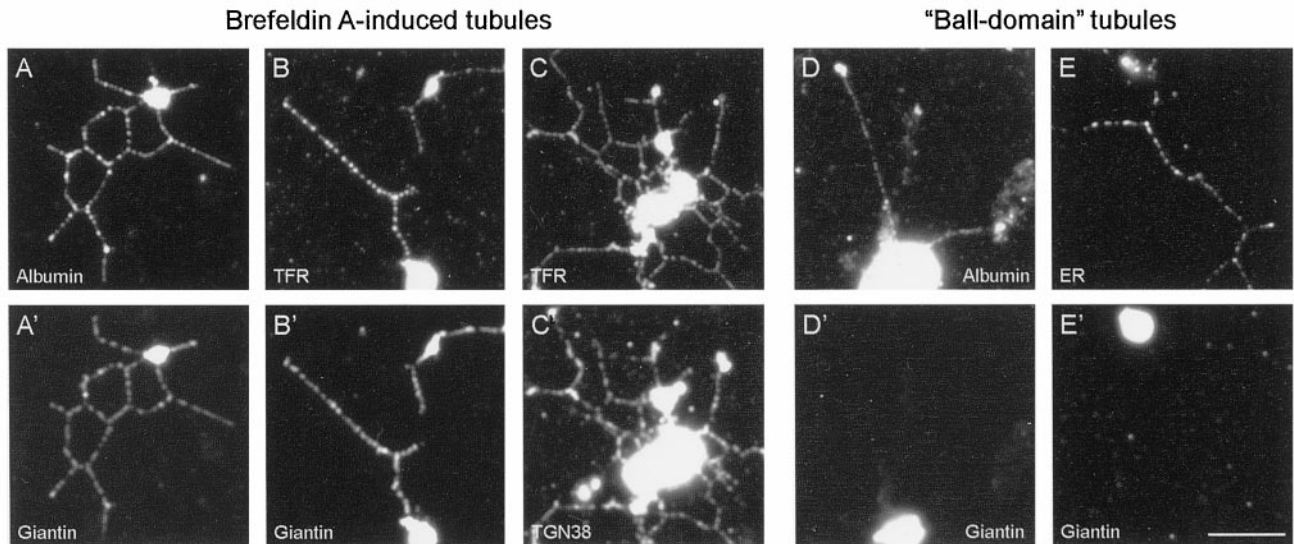
Figure 2. Immunofluorescence analysis of BFA-induced membrane tubules and ball-domain tubules demonstrates that they contain distinct organelle markers. Networks formed in the presence of 100 μg/ml BFA (A–C and A'–C') were processed for double-labeling immunofluorescence (see MATERIALS AND METHODS). The membrane tubules label with antibodies to the secretory marker rat albumin (A), the Golgi stack protein giantin (A' and B'), TGN38 (C'), and transferrin receptor (B and C), demonstrating that fusion has occurred between elements of the Golgi apparatus, TGN, and early endosomes. A different class of membrane tubule, ball-domain tubules, assemble in the absence of BFA when the rat liver Golgi fraction is incubated with *Xenopus* egg cytosol prepared by a different method (Allan and Vale, 1994; see MATERIALS AND METHODS). Unlike BFA tubules, the ball-domain tubules do not contain giantin (D' and E') but do label with antibodies against rat albumin (D) and the mAb 1D3 (E), which recognizes KEDL-containing proteins in the ER. Bar, 5 μm (applies to all panels).

Helms and Rothman, 1992). ADP ribosylation factor is recruited to the Golgi membrane when it is in its GTP-bound form, and it, in turn, recruits the coatomer subunits needed for the formation of COP I-coated vesicles (Orci *et al.*, 1991; Donaldson *et al.*, 1992; Klausner *et al.*, 1992). Because BFA-induced dissociation of coatomer, and therefore membrane tubule formation, is inhibited by pretreatment with the non-hydrolyzable analogue of GTP (GTPγS) (Donaldson *et al.*, 1991), we predicted that similar results should be observed in vitro.

Rat liver Golgi membranes in interphase *Xenopus* egg cytosol were treated with 0.25 mM GTPγS for 5 min at room temperature, followed by 10 min on ice, either before or after the addition of 100 μg/ml BFA. These samples were then flowed into the microscope perfusion chambers and observed by VE-DIC microscopy. Pretreatment of the membranes with GTPγS resulted in a dramatic inhibition of membrane tubule formation in the presence of BFA (Figure 3A). In contrast, when the membranes were incubated with GTPγS after BFA addition, no inhibition of membrane tubule formation was apparent after 10 min in the flow chamber (Figure 3A), and only a limited inhibition was observed after 60 min (Figure 3A). These results suggest that GTPγS does not have a direct effect on BFA tubule motor activity. This is in contrast to the movement of ball-domain tubules, which was completely inhibited (no movements observed during 30 min) by incubation with 0.25 mM GTPγS in the presence or absence of BFA.

The effect of treating the membranes with GTPγS and BFA was then correlated with its effect on the membrane binding of β-COP, a component of the COP I coatomer complex

(Figure 3B). Immunoblotting of rat liver Golgi membranes incubated in buffer alone revealed that rat β-COP is recognized as a single band (lane 5). When membranes were incubated in interphase *Xenopus* egg cytosol (see MATERIALS AND METHODS), an additional band was detected by the anti-β-COP antibody, corresponding to *Xenopus* β-COP that had been recruited to the membrane (lane 1). If BFA was present during the incubation with cytosol, less β-COP (both rat and *Xenopus*) was detected in the membrane pellet (lane 2). However, when membranes and cytosol were preincubated with GTPγS for 5 min before addition of BFA, the amount of membrane-associated β-COP was greatly increased (lane 3). This was not seen if GTPγS was added after BFA (lane 4).

From these results it is clear that in our in vitro assay BFA is having the expected effect on β-COP recruitment, and moreover, that stimulating coatomer recruitment by adding GTPγS was correlated with the prevention of membrane tubule movement and extension.

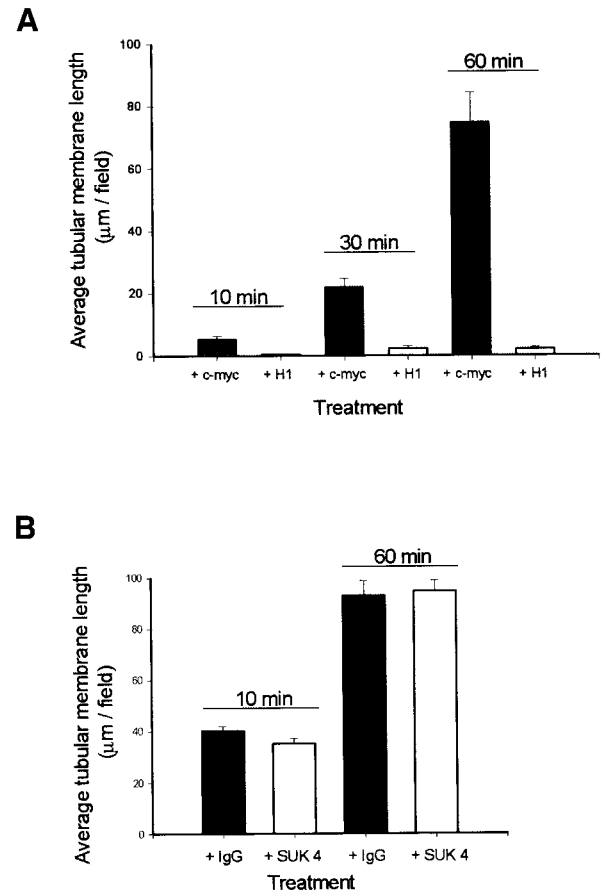### BFA-induced Membrane Tubule Formation Is Inhibited by the H1 Monoclonal Antibody

Having demonstrated that BFA-induced membrane tubule formation is due to microtubule motor activity, an antibody inhibition approach was used to identify candidate motors. The H1 anti-kinesin monoclonal antibody has previously been shown to inhibit BFA-dependent Golgi redistribution in vivo (Lippincott-Schwartz *et al.*, 1995) and was therefore the most obvious candidate to block motor function in this assay.
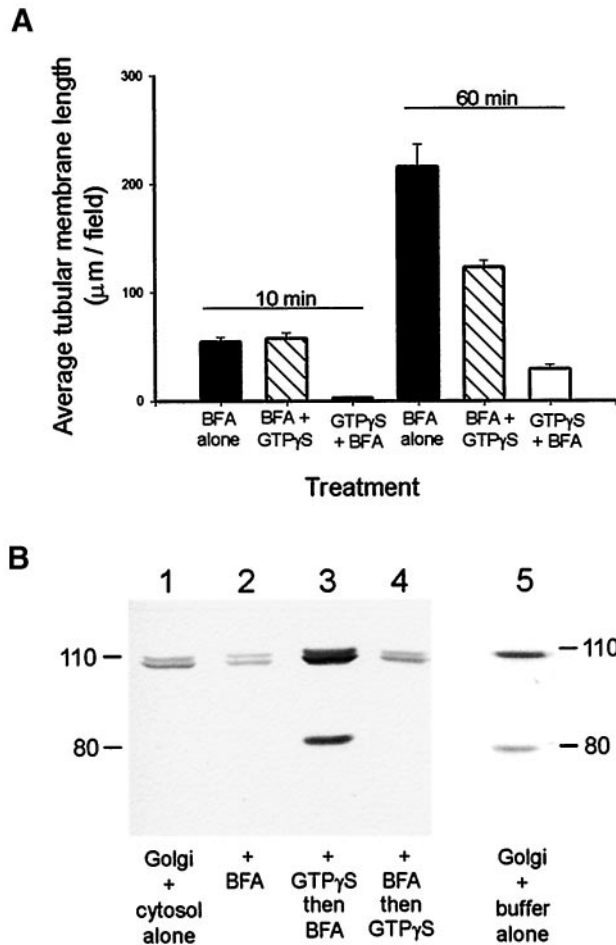
Figure 3. Effect of GTPγS on BFA-induced membrane tubule formation correlated with β-COP membrane binding. (A) The effect of treating rat liver Golgi fraction membranes with GTPγS on BFA-induced membrane tubule formation was assayed. Membranes in interphase cytosol were treated with 0.25 mM GTPγS 15 min before (GTPγS + BFA), or 15 min after (BFA + GTPγS) the addition of BFA or were not treated with GTPγS (BFA alone), and membrane tubule formation was quantitated (see MATERIALS AND METHODS). Membrane tubule formation was averaged over 25 fields. Error bars indicate SEMs. (B) GTPγS treatment was then correlated with the membrane binding of β-COP. Membranes were incubated in interphase cytosol (lane 1 [Golgi + cytosol alone]), or cytosol plus BFA (lane 2 [+ BFA]) for 30 min at room temperature, followed by a 15-min incubation on ice. Alternatively, membranes were incubated with cytosol plus GTPγS for 5 min before the addition of BFA (lane 3 [+ GTPγS then BFA]) and were then incubated as described above. Membranes were also incubated with cytosol plus BFA for 5 min before the addition of GTPγS for a further 30 min at room temperature, followed by 15 min on ice (lane 4 [+ BFA then GTPγS]). Finally, rat liver Golgi membranes were incubated in acetate buffer alone (lane 5 [Golgi + buffer alone]). Membranes were recovered by spinning through a 0.4 M sucrose/acetate buffer cushion and were then subjected to SDS-PAGE and immunoblotting with the maD anti-β-COP antibody. The immunoreactive band at ~80 kDa is a proteolytic fragment of β-COP.

Membranes were preincubated with H1 ascites or with a control anti-c-*myc* ascites for 20 min, as described in MATERIALS AND METHODS, and then added to untreated in-

Figure 4. BFA-induced membrane tubule formation is inhibited by the H1 anti-kinesin monoclonal antibody, but not the SUK 4 anti-kinesin monoclonal antibody. (A) Membranes were preincubated with H1 ascites (+ H1) or with a control anti-c-*myc* ascites (+ c-myc) at a ratio of 5:1 for 20 min on ice. Membranes were then mixed with interphase cytosol and 100 μg/ml BFA and were introduced into perfusion chambers and observed by VE-DIC, and the level of membrane tubule formation was quantitated. Membrane tubule formation was shown to be almost totally inhibited by pretreatment of the membranes with H1. (B) Membranes were preincubated with the SUK 4 anti-kinesin antibody (+ SUK 4) or with a control mouse IgG (+ IgG), and membrane tubule formation was assayed as in A but with the modifications described in MATERIALS AND METHODS. No inhibition of BFA-induced membrane tubule formation was observed as a result of membrane pretreatment with SUK 4. Membrane tubule formation was averaged over 25 fields. Error bars indicate SEMs.

terphase cytosol. Membrane tubule formation was shown to be almost totally inhibited by pretreatment of the membrane with H1 (Figure 4A). Interestingly, H1 treatment had no effect on the amount of vesicle movement observed (Robertson and Allan, unpublished data), which, taken together with the different rates of tubule and vesicle movement, strongly suggested that the two types of translocation involved different plus end–directed motors.

We then repeated the above experiment using a different function-blocking anti-kinesin antibody, SUK 4 (Ingold *et al.*, 1988). Surprisingly, pretreatment of Golgi membranes with
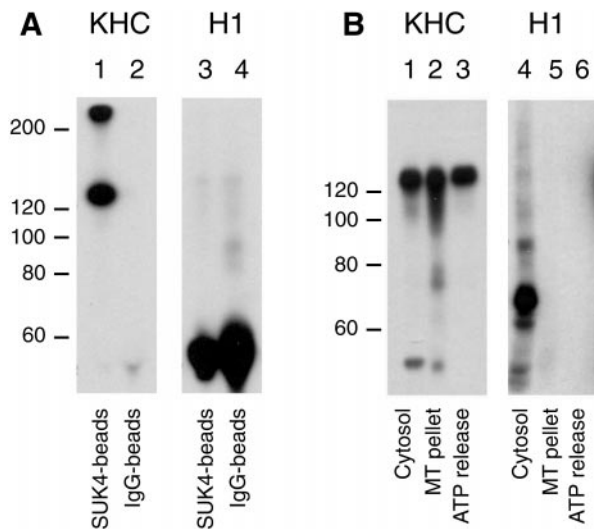
Figure 5. H1 does not recognize conventional KHC in rat liver Golgi membranes or in *Xenopus* egg cytosol. (A) Ubiquitous kinesin immunoprecipitated from solubilized rat liver Golgi membranes using the SUK 4 monoclonal (lanes 1 and 3) was immunoblotted with either polyclonal anti-uKHC (lane 1), which recognized bands at ~125 and ~250 kDa (probably incompletely dissociated kinesin heavy chains), or H1 (lane 3), which failed to produce a signal. Nonimmune mouse IgG was used as a control (lanes 2 and 4). The bands between 50 and 60 kDa are antibody heavy chains (lanes 3 and 4). (B) Microtubule pellets enriched in motors were prepared from interphase *Xenopus* egg cytosol and then extracted with 5 mM ATP and 100 mM NaCl to give an ATP release fraction (lanes 3 and 6) and the remaining microtubule pellet (lanes 2 and 5). Interphase cytosol is loaded in lanes 1 and 4. After SDS-PAGE, protein samples were immunoblotted with either the polyclonal anti-uKHC antibody (lanes 1–3) or the H1 monoclonal antibody (lanes 4–6). Although H1 recognized a band at ~70 kDa (lane 4), this polypeptide did not pellet with microtubules, unlike uKHC (compare lanes 2 and 3 with 5 and 6).

SUK 4 failed to cause any inhibition of membrane tubule formation (Figure 4B), even in cytosol that had been immunodepleted of kinesin (Robertson and Allan, unpublished data). The same preparation of SUK 4, used at the same dilution, effectively inhibited plus end–directed ER tubule extensions in vitro (Lane and Allan, 1999), demonstrating that our antibody preparation was functional.

Ubiquitous Kinesin Heavy Chain Is Not the Motor Involved in BFA-induced Membrane Tubule Formation

The apparent conflict between the results obtained after H1 and SUK 4 anti-kinesin antibody treatments led us to investigate which polypeptides the antibodies were recognizing in *Xenopus* egg cytosol and the rat liver Golgi fraction. We have previously shown that SUK 4 recognizes *Xenopus* egg kinesin (Lane and Allan, 1999). Although the SUK 4 antibody did not recognize any polypeptides by immunoblotting of the Golgi membranes (Robertson and Allan, unpublished data), it did immunoprecipitate conventional uKHC efficiently from solubilized membranes (Figure 5A, lane 1),
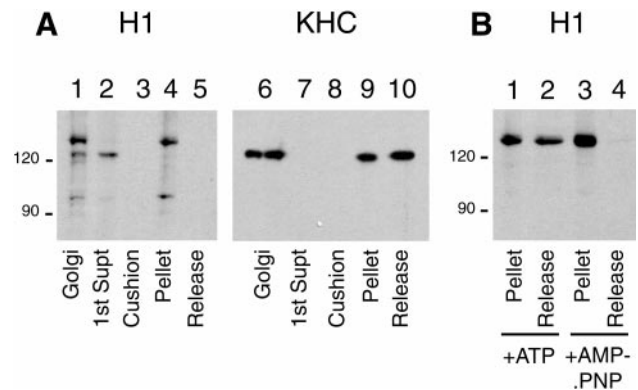
Figure 6. Identification of candidate motor proteins for BFA-induced membrane tubule formation. (A) Biochemical analysis of motor and microtubule binding. Rat liver Golgi membranes were solubilized and incubated with microtubules under conditions that promote motor binding. Microtubules were recovered by centrifugation, and the proteins present in the remaining supernatant fraction (lane 2 and 7) and the cushion fraction (lane 3 and 8) were recovered by precipitation. The microtubule pellet was resuspended in buffer containing 5 mM ATP and 100 mM KCl and centrifuged to give a microtubule pellet (lanes 4 and 9) and an ATP release supernatant (lanes 5 and 10). Untreated Golgi fraction was loaded in lanes 1 and 6. After SDS-PAGE, protein samples were immunoblotted with either the H1 monoclonal antibody (lanes 1–5) or the polyclonal anti-uKHC antibody (lanes 6–10). (B) Microtubule pellets with rigor-bound motors were incubated with buffer containing 0.5 M NaCl plus either 5 mM ATP (lanes 1 and 2) or 5 mM AMP.PNP (lanes 3 and 4). Microtubule pellets (lanes 1 and 3) and release fractions (lanes 2 and 4) were resolved by SDS-PAGE and immunoblotted with the H1 antibody.

as detected using a polyclonal antibody to uKHC (Niclas *et al.*, 1994).

H1 is known to recognize bovine brain KHC (Pfister *et al.*, 1989) and labels purified bacterially expressed rat uKHC head domain by immunoblot (Robertson and Allan, unpublished data). However, H1 did not recognize *Xenopus* uKHC but instead detected only a polypeptide of ~70 kDa in *Xenopus* egg extracts (Figure 5B, lane 4) that was unable to bind to microtubules (lanes 5 and 6), making this protein an unlikely candidate for the motor involved in driving membrane tubule formation. In addition, H1 only inhibited tubule extension when it was preincubated with membranes (Figure 4A) and not when it was added first to the cytosol (Robertson and Allan, unpublished data). The ~70-kDa protein in *Xenopus* cytosol is therefore likely to be recognized by H1 because of antibody cross-reaction.

Because all the functional evidence pointed to the motor protein being present on the membranes, we investigated which proteins H1 recognized in the Golgi fraction. Surprisingly, H1 revealed not only a band at M_r ~124,000, which had a mobility similar to that of the polypeptide recognized by a polyclonal anti-uKHC antibody (Figure 6A, lane 6), but also proteins at M_r ~130,000 and ~100,000 (Figure 6A, lane 1), although the intensity of the ~100-kDa immunoreactive band varied somewhat between preparations. It was therefore necessary to establish whether any of these bands were microtubule motors. One of the characteristic properties of KLPs is that they bind rigorously to microtubules under

conditions of ATP depletion, in the presence of the nonhy-drolyzable ATP analogue AMP.PNP. This trait was used to establish whether the H1 antigens identified in the Golgi fraction behaved like KLPs in a biochemical assay.

Detergent-solubilized membranes were incubated with microtubules in the presence of AMP.PNP under conditions that cause ATP depletion (see MATERIALS AND METH-ODS) for 25 min at room temperature. The microtubules were then recovered by centrifugation, and the microtubule pellet was carefully resuspended and incubated in buffer containing 5 mM ATP and 100 mM KCl. The microtubules were then separated from the released motor fraction by centrifugation. The resultant microtubule pellet and ATP release supernatant were resolved by SDS-PAGE and immu-noblotted with H1 (Figure 6A, lanes 4 and 5) or the anti-uKHC polyclonal antibody (Figure 6A, lanes 9 and 10). The proteins that remained in the supernatant and cushion dur-ing the first spin were recovered by precipitation (see MA-TERIALS AND METHODS) and analyzed in parallel (Figure 6A, lanes 2, 3, 7, and 8).

Immunoblotting revealed, unexpectedly, that the H1 an-tigen that comigrated with kinesin heavy chain by SDS-PAGE did not associate with microtubules under conditions that promote motor binding (i.e., in the presence of AMP-.PNP and in the absence of ATP) but instead remained in the supernatant (Figure 6A, lane 2). This band was not detect-able in the cushion, microtubule pellet, or ATP release su-pernatant (Figure 6A, lanes 3–5). Kinesin heavy chain, how-ever, detected using a polyclonal anti-uKHC, behaved exactly as expected: it bound to microtubules under motor binding conditions and was partially released upon treat-ment with ATP and 100 mM KCl (Figure 6A, lanes 9 and 10). Moreover, unlike H1, anti-uKHC did not detect any protein in the postmicrotubule supernatant, suggesting that for some reason H1 does not recognize uKHC in the rat liver Golgi membrane fraction. Further strong evidence for this conclusion was obtained by immunoprecipitating kinesin from solubilized membranes using SUK 4 and probing the precipitates with both the polyclonal anti-uKHC and H1 (Figure 5A, compare lanes 1 and 3).

Identification of Two Candidate Motor Proteins Using the H1 Monoclonal Antibody

We next turned our attention to the other polypeptides detected by the H1 antibody. Both the M_r ~130,000 and ~100,000 bands did indeed bind to microtubules under motor binding conditions (Figure 6A, lane 4), but neither protein was released after ATP and 100 mM KCl treatment (Figure 6A, lane 5). However, because the microtubule mo-tor protein Eg5 (Sawin et al., 1992) is only fully released from the microtubule pellet under more rigorous salt conditions, we repeated the microtubule binding/ATP release experi-ment with the ATP release step carried out in the presence of 0.5 M NaCl instead of 100 mM KCl (Figure 6B, lanes 1 and 2). As a control, ATP was substituted with AMP.PNP, which should prevent motor protein release under these high-salt conditions (Figure 6B, lanes 3 and 4; note that very little of the ~100-kDa band was detected in this preparation). The ~130-kDa antigen was partially released from the microtu-bule pellet under conditions of high salt and ATP (Figure 6B, lane 2), and as would be expected from a KLP, this release
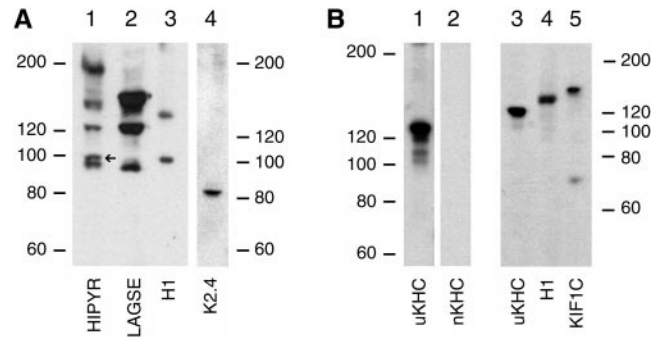
Figure 7. Analysis of the Golgi microtubule motor fraction with a range of antibodies to kinesin superfamily members. (A) Concen-trated microtubule plus motor pellets were prepared from rat liver Golgi membranes (see MATERIALS AND METHODS) and immu-noblotted with antibodies against HIPYR (lane 1), LAGSE (lane 2), H1 (lane 3), or K2.4 (lane 4), which recognizes the 85-kDa compo-nent of kinesin II. The microtubule motors were isolated from the following amounts of Golgi membrane protein: lanes 1 and 2, 3 mg; lane 3, 600 μg; and lane 4, 1.2 mg. (B) Microtubule motor protein fractions prepared from 500 μg of Golgi membrane protein were analyzed by immunoblotting. Although these motor fractions con-tained uKHC (lanes 1 and 3), no signal was detected using affinity-purified anti-nKHC (lane 2). Both uKHC (lane 3) and KIF1C (lane 5) migrate with different mobilities to the ~130-kDa H1 antigen.

was prevented when ATP was substituted with AMP.PNP (Figure 6B, lane 4).

Another feature that has helped in the identification of a number of KLPs is the fact that antibodies generated to conserved sequences with the motor domain will recoginze a fairly broad range of kinesin family members (e.g., Cole et al., 1992; Sawin et al., 1992). We therefore immunblotted the Golgi-derived motor fractions with affinity-purified anti-LAGSE and anti-HIPYR (Sawin et al., 1992), and, as has been observed previously (Sawin et al., 1992), the polypeptides recognized by each antibody were mostly distinct, with only some being recognized by both reagents (Figure 7, lanes 1 and 2). The ~100-kDa H1 antigen (lane 3) comigrated with a polypeptide labeled by the HIPYR (lane 1, arrow), but not LAGSE (lane 2) antibodies, providing further evidence that it is a member of the kinesin superfamily. There was no clear immunoreactive band in either the HIPYR or LAGSE lanes that comigrated with ~130-kDa H1 antigen, although the strength of the signal at ~150 kDa in the LAGSE lane could have masked such a signal. It should be stressed that these antibodies, even taken together, do not recognize all KLPs. This is shown clearly by the observation that we could demonstrate the presence of the 85-kDa component of kine-sin II using a monoclonal antibody (Figure 7, lane 4), even though neither HIPYR nor LAGSE antibodies recognized proteins in this size range in the Golgi motor preparation (lanes 1 and 2).

So far, four kinesin family members have been implicated in Golgi complex membrane dynamics, namely, kinesin heavy chain (Feiguin et al., 1994; Lippincott-Schwartz et al., 1995), Rabkinesin 6 (Echard et al., 1998), kinesin II/Xklp3/ KIF3C (Le Bot et al., 1998; Yang and Goldstein, 1998), and KIF1C (Dorner et al., 1998). Having compiled evidence that the ~100- and ~130-kDa H1 antigens are motor proteins, it

was necessary to establish whether they corresponded to any of these candidate Golgi motors.

Microtubule pellets enriched in Golgi membrane motors were immunoblotted with antibodies against kinesin heavy chain (Figure 7B, lanes 1 and 3) and KIF1C (Figure 7B, lane 5), neither of which recognized bands that comigrated with either H1 antigen (Figure 7, A, lane 3, and B, lane 4). In addition, both antigens are larger than the 85- and 95-kDa kinesin II subunits. It was possible that the ~130-kDa H1 antigen was an isoform of KHC, even though all such isoforms described so far are neuronally enriched. However, an affinity-purified antibody against nKHC (Niclas *et al.*, 1994) did not recognize any polypeptides in this Golgi-derived microtubule motor fraction (Figure 7B, lane 2).

One obvious candidate of ~100 kDa is Rabkinesin 6, but a number of lines of evidence suggest that this protein is not the ~100-kDa H1 antigen. First, an antibody against Rabkinesin 6 (Echard *et al.*, 1998) did not recognize any proteins of the appropriate size in the rat liver Golgi membrane or motor fraction by immunoblotting (Robertson and Allan, unpublished data). Second, inspection of the Rabkinesin 6 sequence (Echard *et al.*, 1998) revealed that anti-LAGSE, but not anti-HIPYR, would be expected to recognize this motor, exactly the reverse of what we found for the H1 antigen. Moreover, neither bacterially nor baculovirally expressed Rabkinesin 6 was labeled by H1 (Goud, personal communication).

Taken together these results indicate that both the ~100- and ~130-kDa H1 antigens represent motors not previously implicated in the movement of Golgi membranes. Unfortunately, attempts to obtain peptide sequence data from the ~130-kDa band have so far been unsuccessful.

BFA-induced Membrane Networks Do Not Form in Metaphase Cytosol

There is considerable evidence that both membrane traffic and many types of organelle movement are inhibited as cells enter metaphase (reviewed in Robertson and Allan, 1997), and we have previously made use of the *Xenopus* egg extract system to investigate metaphase regulation of membrane motility (e.g., Allan and Vale, 1991; Niclas *et al.*, 1996). We therefore investigated whether BFA-induced membrane tubule formation was similarly regulated within the context of the cell cycle by comparing the levels of membrane tubule formation in metaphase cytosol versus interphase cytosol.

Interphase extracts were made by activating a metaphase-arrested extract with Ca^{2+} in the presence of cycloheximide, which results in a release of the metaphase block and drives the extract into an interphase state. Metaphase-arrested extracts were mock activated (see MATERIALS AND METHODS). The cell cycle status of these respective extracts was confirmed by assaying the level of histone H1 phosphorylation (Robertson and Allan, unpublished data). Histone H1 is a substrate for the mitotic kinase p34cdc2 and can therefore be used to elucidate the level of mitotic kinase activity in an extract (Murray, 1991; Allan, 1998).

First, we established that substituting metaphase for interphase cytosol had no effect on the ability of BFA to interfere with the membrane binding of β-COP (Robertson and Allan, unpublished data). We then used VE-DIC to monitor whether BFA tubules formed in the presence of metaphase cytosol. Initial observations revealed that sub-
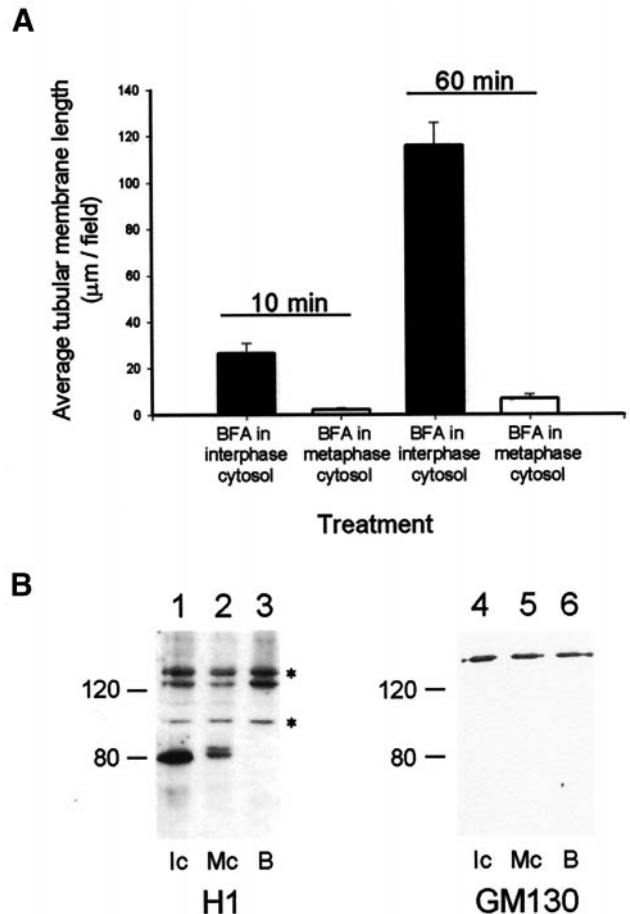
Figure 8. Analysis of the cell cycle regulation of BFA-induced membrane tubule formation and H1 motor membrane association. (A) The amount of BFA-induced membrane tubule formation in interphase versus metaphase cytosols was compared. Interphase extracts were made by activating metaphase-arrested extracts with Ca^{2+} in the presence of cycloheximide (see MATERIALS AND METHODS). Motility assays and quantitation were carried out as before, except that 40 μM sodium orthovanadate was included to inhibit the microtubule gliding seen in metaphase-arrested extracts. Membrane tubule formation was averaged over 25 fields. Error bars indicate SEMs. (B) The membrane binding of the ~130- and ~100-kDa H1 antigens (*) was assessed after incubation in interphase and metaphase cytosol. Rat liver Golgi membranes were incubated in interphase cytosol (lanes 1 and 4), metaphase cytosol (lane 2 and 5), or acetate buffer without sucrose (lane 3 and 6), as described in MATERIALS AND METHODS. Membranes were recovered by spinning through a 0.4 M sucrose/acetate buffer cushion and were subjected to SDS-PAGE and immunoblotting with either the H1 monoclonal antibody (left panel) or an anti-GM130 polyclonal antibody (as a loading control [right panel]).

stantially fewer tubules were extended in metaphase cytosol, but on closer inspection it was clear that almost all such tubules were extending via attachment to cytoplasmic dynein-driven gliding microtubules (which are seen far more frequently in metaphase compared with interphase cytosols) and were not due to membrane-associated micro-

tubule motor activity. To simplify analysis of membrane tubule extension by ensuring that only genuine membrane motor activity was counted, cytoplasmic dynein activity was inhibited by including 40 μM sodium orthovanadate, a treatment that did not affect tubule formation in interphase cytosol (Figure 8A). Under these conditions it was found that the formation of BFA-induced tubular membrane networks was not supported in metaphase cytosol (Figure 8A).

The Membrane Binding of the ~130- and ~100-kDa H1 Antigens Is Not Altered as a Result of Incubation in Metaphase Cytosol

There are three possible mechanisms by which the microtubule motor-driven motility of the BFA-induced membrane tubules could be inhibited in metaphase. First, the binding of the motor to the membrane may be controlled directly, so that inhibition of tubule movement corresponds to the motor becoming detached from the membrane. Second, motor binding may remain constant, whereas the ATPase activity of the bound motor is down-regulated. Finally, the microtubule may be modified in some way so that the motor can no longer move along its surface. We therefore tested what happened to the two candidate motors for BFA-induced membrane tubule formation when rat liver Golgi membranes were incubated in interphase cytosol (Figure 8B, lanes 1 and 4), metaphase cytosol (Figure 8B, lanes 2 and 5), or buffer (Figure 8B, lanes 3 and 6) and then pelleted by centrifugation through a sucrose cushion. Immunoblotting with an antibody against a Golgi resident protein, GM130, demonstrated that equal amounts of rat liver Golgi membranes were recovered under all conditions (Figure 8, lanes 4–6), with the maximum variation in band intensity being 4.4%.

Immunoblotting with the H1 antibody also revealed only small differences in the amount of the ~130- and ~100-kDa antigens attached to the membranes after incubation in either cytosol (Figure 8B, compare lanes 1 and 2). Analysis of band intensity revealed a ~25% reduction of ~130-kDa motor and an 8% reduction in ~100-kDa motor binding in metaphase cytosol compared with interphase cytosol. Given that there the amount of membrane-associated ~130- and ~100 kDa antigens remained broadly similar, whereas membrane motility was reduced by up to ~1700%, it is therefore unlikely that an inhibition of membrane binding is the regulatory mechanism in metaphase.

DISCUSSION

Treatment of living cells with BFA results in the formation of a variety of membrane tubules, including those that move out from the Golgi apparatus and fuse with the ER (Lippincott-Schwartz et al., 1989, 1990; Sciaky et al., 1997) and those that extend from the TGN and early endosome, which then fuse with each other (Lippincott-Schwartz et al., 1991; Wood et al., 1991). Although in vivo studies have established a role for microtubule motor protein activity in BFA tubule extension (Lippincott-Schwartz et al., 1990, 1991, 1995; Wood et al., 1991; Reaves and Banting, 1992), they do not easily allow a more detailed analysis of the properties and regulation of the motor protein involved. In this study, therefore, we have reconstituted BFA-induced membrane tubule formation in

vitro in an assay that permits the observation of motor protein activity, coupled with a correlative biochemical analysis.

We have shown that when rat liver Golgi membranes are incubated in interphase *Xenopus* egg cytosol in the presence of BFA, an intricate network of interconnected membrane tubules is formed. One notable feature of the in vitro BFA tubules is that they contain markers for the Golgi stack, TGN, and early endosomes, suggesting that the membrane fusion events occuring in vitro have a broader specificity than those seen in studies in vivo. This may reflect the fact that these compartments may be in closer contact within the membrane aggregates in the Golgi fraction than they would normally be within the cell. However, it is also possible that there is a low level of Golgi stack–TGN–early endosome fusion that occurs in vivo in the presence of BFA that has gone unnoticed. This might not be surprising given that toxins such as Shiga toxin are able to traffic from the cell surface back to the ER, via the endosome and Golgi apparatus (e.g., Johannes et al., 1997).

Although the in vitro BFA networks contain a mixture of Golgi stack, TGN, and early endosomal markers, there are a number of features of both our results and those of others that, taken together, strongly suggest that we are looking at the motor activity that drives tubule extension from the Golgi stack, rather than from the TGN or endosomes. First, H1 inhibits the redistribution of the medial Golgi marker mannosidase II in vivo (Lippincott-Schwartz et al., 1995), and the same reagent blocks BFA tubule formation in our assay. Second, we have found that the function-blocking anti-uKHC antibody SUK 4 does not inhibit tubule motility in vitro. Also, abrogating kinesin function in vivo using a variety of approaches, including the generation of null uKHC mice (Tanaka et al., 1998), antisense suppression of uKHC expression (Feiguin et al., 1994), and expression of uKHC ATPase-defective mutants (Nakata and Hirokawa, 1995), all have no effect on the redistribution of Golgi stack markers to the ER after BFA treatment. Importantly, KHC antisense suppression did inhibit the formation of endosomal and TGN-derived BFA tubules (Feiguin et al., 1994). The same approaches (Feiguin et al., 1994; Nakata and Hirokawa, 1995; Tanaka et al., 1998; Wubbolts et al., 1999) (reviewed in Lane and Allan, 1998) and that of SUK 4 microinjection (Tuma et al., 1998) also all resulted in an inhibition of plus end–directed lysosome and/or late endosome movement. It seems likely, therefore, that although conventional kinesin moves endocytic organelles, and possibly TGN elements, it does not drive Golgi-to-ER traffic. The latter transport step is driven instead by a motor that is inhibited by H1, and we think it highly likely that we have reconstituted this motile event in vitro.

Membrane tubule networks have also been seen previously to form from these rat liver membranes in the absence of BFA (Allan and Vale, 1994). We have presented evidence that strongly suggests that the two types of membrane networks are different, based on morphological criteria and immunofluorescence data (Figure 2), and that distinct motors drive the motility, based on the rates of movement of the two tubule types and the sensitivity of the motors involved to GTPγS. The crucial difference that determines whether ball-domain tubules form in the absence of BFA

seems to be the method used to prepare the *Xenopus* egg cytosol. Why this should be is currently completely unclear.

Interestingly, Fullerton *et al.* (1998) observed similar ball-domain tubular networks extending from rat liver Golgi fractions in the presence of rat liver cytosol, but in this situation the H1 antibody inhibits the motility of both membrane tubules and vesicles (Fullerton *et al.*, 1998), which move four times faster than BFA tubules. It is, of course, possible that the antibody is inhibiting the same motor on both ball-domain and BFA tubules but that the different cytosolic conditions result in differences in motor behavior. The other more likely possibility, supported by the biochemical data presented here, is that H1 recognizes and inhibits a number of active motor proteins (at least two). Another function-blocking antibody raised against conventional kinesin, the HD antibody (Rodionov *et al.*, 1991), has since been found to inhibit other KLPs (Wright *et al.*, 1993; Lombillo *et al.*, 1995), and recent evidence suggests that the HD antibody also inhibits kinesin II (Tuma *et al.*, 1998).

The H1 antibody was raised against bovine brain kinesin (Bloom *et al.*, 1988) and recognizes bacterially expressed rat kinesin heavy chain head domain (Robertson and Allan, unpublished data). However, the H1 antigen in the Golgi motor fraction that migrates with a similar mobility to that of uKHC surprisingly did not bind to microtubules under conditions of ATP depletion (Figure 6). Moreover, uKHC immunoprecipitated from the Golgi motor fraction was also not recognized by H1 (Figure 5). This suggests that the ~124-kDa protein that H1 recognizes in these fractions is a nonmotor protein, which just happens to comigrate with conventional kinesin. Two formal possibilities are that H1 only reacts with a post-translationally modified form of uKHC or with one of the other identified KHC isoforms (all neuronally expressed). We think the former is unlikely based on our experiments using both a polyclonal anti-uKHC and the SUK 4 monoclonal anti-uKHC (Figures 5–7), and the latter possibility was ruled out using an affinity-purified antibody to nKHC (Niclas *et al.*, 1994).

The fact that pretreating the rat liver Golgi membranes with H1 inhibits BFA-induced membrane tubule formation in *Xenopus* egg cytosol implies that the motor responsible is an active rat motor. H1 recognizes two bands in a motor fraction prepared from rat liver Golgi membranes, which both behave like a number of kinesin-like proteins in a biochemical assay and which migrate at ~100 and ~130 kDa. The smaller of these two polypeptides also comigrates with a band that is labeled by an antibody raised against a conserved sequence in the kinesin family motor domain (anti-HIPYR; Sawin *et al.*, 1992). These results suggest that either the ~130- or ~100-kDa antigen, and not conventional kinesin, is the motor responsible for driving membrane tubule formation as a result of BFA treatment in vitro. This is supported by the observation that the SUK 4 anti-kinesin heavy chain monoclonal antibody does not inhibit BFA-induced membrane tubule formation in our assay, whereas it does inhibit plus end–directed ER movement under similar experimental conditions (Lane and Allan, 1999).

Three KLPs have been implicated in Golgi membrane dynamics so far: Rabkinesin 6 (Echard *et al.*, 1998), kinesin II (Le Bot *et al.*, 1998; Yang and Goldstein, 1998), and KIF1C (Dorner *et al.*, 1998) have all been localized to the Golgi apparatus or associated membranes (either by immunofluoresence or by immunoelectron microscopy). Overexpression of Rabkinesin 6 causes the fragmentation of the Golgi apparatus (Echard *et al.*, 1998), whereas overexpression of an inactive form of KIF1C appears to inhibit BFA-induced Golgi redistribution (Dorner *et al.*, 1998). KIF3C (Yang and Goldstein, 1998) and Xklp3 (Le Bot *et al.*, 1998), both of which are members of the kinesin II family, have also been localized to the Golgi apparatus. However, after BFA treatment, Xklp3 was localized to dispersed vesicles positive for the KDEL receptor. These structures do not redistribute to the ER after BFA treatment and are thought to represent a recycling compartment between the ER and Golgi apparatus (Le Bot *et al.*, 1998). All of these proteins (kinesin II/Xklp3/KIF3C, Rabkinesin 6, and KIF1C) together with conventional kinesin migrate at different molecular masses to the ~130-kDa motor that we have now identified using the H1 monoclonal antibody, which suggests that at least five different kinesin family members could be involved in the maintenance of normal Golgi structure and function. The ~100-kDa motor has a molecular mass very similar to that of Rabkinesin 6, but a number of features strongly suggest that it is a distinct protein. First, bacterially expressed and baculovirus-expressed Rabkinesin 6 is not recognized by H1 (Goud, personal communication). Second, the Rabkinesin 6 sequence possesses a good LAGSE consensus sequence, but not a HIPYR sequence; in contrast, the ~100-kDa motor described here comigrates with a band that labels with anti-HIPYR but not anti-LAGSE. Clearly, the way forward is to obtain the sequences of both the ~100- and ~130-kDa motors.

So why are so many plus end–directed motors required within the same organelle? The key to this question could lie in the organization of the microtubule array in animal cells. Microtubules are oriented with their plus ends outermost and their minus ends at the microtubule-organizing center, which is located at the center of the cell, near the nucleus. In interphase, the Golgi apparatus is typically clustered around the microtubule-organizing center, and its position is thought to be maintained by the minus end–directed motor cytoplasmic dynein (Burkhardt *et al.*, 1997; Presley *et al.*, 1997; Lane and Allan, 1998). Microtubule-mediated transport from the Golgi apparatus to more peripheral intracellular sites would therefore require the action of a plus end–directed motor protein. It is likely that a number of distinct transport steps originate from the Golgi apparatus and are directed toward the cell periphery (including transport from the Golgi to the ER, TGN to the plasma membrane, and TGN to the endocytic pathway). Bearing in mind the polar organization of the Golgi apparatus, Golgi-to-ER transport may consist of more than one transport process with, for example, transport from the *cis*-Golgi to the ER being distinct from transport from the medial- or *trans*-Golgi to the ER. The existence of these multiple transport steps may well explain the presence of multiple KLPs on the Golgi apparatus, with each motor being responsible for a particular transport process, thus permitting the differential regulation of each motor.

The regulation of motors at various stages of the cell cycle is of particular interest when considering the Golgi

apparatus, because of the dramatic change in Golgi morphology that occurs during cell division. During the transition from interphase to mitosis, the Golgi apparatus fragments and vesiculates to become scattered throughout the cell (Robbins and Gonatas, 1964; Lucocq and Warren, 1987), thus ensuring an even distribution of Golgi components between the two daughter cells. Given that the Golgi apparatus interacts readily with microtubules in interphase (Rogalski and Singer, 1984), it is possible that an inhibition of microtubule-based Golgi motility during mitosis could aid mitotic Golgi redistribution. Indeed, in experiments using the expression of *N*-acetyl glucosamine transferase I (a resident Golgi apparatus enzyme) tagged with green fluorescent protein as a marker for the Golgi apparatus in vivo, it has been shown that mitotic Golgi fragments are actively scattered during prophase and prometaphase and are able to remain attached to microtubules but cannot move along them during metaphase (Shima *et al.*, 1997, 1998). It would be surprising then if metaphase *Xenopus* egg cytosol did support BFA-induced membrane tubule formation.

There are three basic models for how motor-dependent organelle movement might be regulated. First, the binding of motor to its cargo may be modulated, so that organelle movement is inhibited by the motor responsible becoming detached from the membrane. This appears to be the case for the inhibition of cytoplasmic dynein-driven ER movement in metaphase *Xenopus* egg cytosol (Allan and Vale, 1991; Niclas *et al.*, 1996). Second, motor binding may remain constant while the ATPase activity of the bound motor is regulated. Third, the microtubule may be modified in some way so that the motor can no longer move along its surface (e.g., Bulinski *et al.*, 1997). The fact that the level of membrane-associated ~130- and ~100-kDa motors differs little between interphase and metaphase cytosols suggests that regulation is via one of the latter two mechanisms.

ACKNOWLEDGMENTS

REFERENCES

Allan, V. (1993). Assay of membrane motility in interphase and metaphase *Xenopus* extracts. In: Methods in Cell Biology, ed. J.M. Scholey, San Diego: Academic Press, 203–226.

Allan, V. (1998). Organelle motility and membrane network formation in metaphase and interphase cell-free extracts. Methods Enzymol. *298*, 339–53.

Allan, V., and Vale, R.D. (1991). Cell cycle control of microtubule-based membrane transport and tubule formation in vitro. J. Cell Biol. *113*, 347–359.

Allan, V., and Vale, R. (1994). Movement of membrane tubules along microtubules in vitro: evidence for specialized sites of motor attachment. J. Cell Sci. *107*, 1885–1897.

Bloom, G.S., Wagner, M.C., Pfister, K.K., and Brady, S.T. (1988). Native structure and physical properties of bovine brain kinesin and identification of the ATP-binding subunit polypeptide. Biochemistry *27*, 3409–3416.

Bulinski, J.C., McGraw, T.E., Gruber, D., Nguyen, H.L., and Sheetz, M.P. (1997). Overexpression of MAP4 inhibits organelle motility and trafficking in vivo. J. Cell Sci. *110*, 3055–3064.

Burkhardt, J., Echeverri, C., Nilsson, T., and Vallee, R. (1997). Overexpression of the Dynamitin (p50) subunit of the dynactin complex disrupts dynein-dependent maintenance of membrane organelle distribution. J. Cell Biol. *139*, 469–484.

Cole, D.G., Cande, W.Z., Baskin, R.J., Skoufias, D.A., Hogan, C.J., and Scholey, J.M. (1992). Isolation of a sea urchin egg kinesin-related protein using peptide antibodies. J. Cell Sci. *101*, 291–301.

Cole, D.G., Chinn, S.W., Wedaman, K.P., Hall, K., Vuong, T., and Scholey, J.M. (1993). Novel heterotrimeric kinesin-related protein purified from sea urchin eggs. Nature *366*, 268–270.

Donaldson, J.G., Finazzi, D., and Klausner, R.D. (1992). Brefeldin A inhibits Golgi membrane-catalyzed exchange of guanine nucleotide onto ARF protein. Nature *360*, 350–352.

Donaldson, J.G., Lippincott-Schwartz, J., and Klausner, R.D. (1991). Guanine nucleotides modulate the effects of brefeldin A in semipermeable cells: regulation of the association of a 110-kD peripheral membrane protein with the Golgi apparatus. J. Cell Biol. *112*, 579–588.

Dorner, C., Ciossek, T., Muller, S., Moller, N.P.H., Ullrich, A., and Lammers, R. (1998). Characterization of KIF1C, a new kinesin-like protein involved in vesicle transport from the Golgi apparatus to the endoplasmic reticulum. J. Biol. Chem. *273*, 20267–20275.

Echard, A., Jollivet, F., Martinez, O., Lacapère, J.-J., Rousselet, A., Janoueix-Lerosey, I., and Goud, B. (1998). Interaction of a Golgi-associated kinesin-like protein with Rab6. Science *279*, 580–585.

Elluru, R.G., Bloom, G.S., and Brady, S.T. (1995). Fast axonal transport of kinesin in the rat visual system: functionality of kinesin heavy chain isoforms. Mol. Biol. Cell *6*, 21–40.

Feiguin, F., Ferreira, A., Kosik, K.S., and Caceres, A. (1994). Kinesin-mediated organelle translocation revealed by specific cellular manipulations. J. Cell Biol. *127*, 1021–1039.

Fullerton, A.T., Bau, M.-Y., Conrad, P.A., and Bloom, G.S. (1998). In vitro reconstitution of microtubule plus end-directed, GTPγS-sensitive motility of Golgi membranes. Mol. Biol. Cell *9*, 2699–2714.

Helms, J.B., and Rothman, J.E. (1992). Inhibition by brefeldin A of a Golgi membrane enzyme that catalyzes exchange of guanine nucleotide bound to ARF. Nature *360*, 352–354.

Hirokawa, N., Pfister, K.K., Yorifuji, H., Wagner, M.C., Brady, S.T., and Bloom, G.S. (1989). Submolecular domains of bovine brain kinesin identified by electron microscopy and monoclonal antibody decoration. Cell *56*, 867–878.

Ingold, A.L., Cohn, S.A., and Scholey, J.M. (1988). Inhibition of kinesin-driven microtubule motility by monoclonal antibodies to kinesin heavy chains. J. Cell Biol. *107*, 2657–2667.

Johannes, L., Tenza, D., Antony, C., and Goud, B. (1997). Retrograde transport of KDEL-bearing B-fragment of Shiga toxin. J. Biol. Chem. *272*, 19554–19561.

Klausner, R., Donaldson, J., and Lippincott-Schwartz, J. (1992). Brefeldin A: insights into the control of membrane traffic and organelle structure. J. Cell Biol. *116*, 1071–1080.

Lane, J., and Allan, V. (1998). Microtubule-based membrane movement. Biochim. Biophys. Acta *1376*, 27–55.

Lane, J.D., and Allan, V.J. (1999). Microtubule-based ER motility in *Xenopus* laevis: activation of membrane-associated conventional kinesin during development. Mol. Biol. Cell *10*, 1909–1922.

Le Bot, N., Antony, C., White, J., Karsenti, E., and Vernos, I. (1998). Role of xklp3, a subunit of the *Xenopus* kinesin II heterotrimeric complex, in membrane transport between the endoplasmic reticulum and the Golgi apparatus. J. Cell Biol. 143, 1559–1573.

Leelavathi, D.E., Estes, L.W., Feingold, D.S., and Lombardi, B. (1970). Isolation of a Golgi-rich fraction from rat liver. Biochim. Biophys. Acta *211*, 124–138.

Linstedt, A., and Hauri, H.-P. (1993). Giantin, a novel conserved Golgi membrane protein containing a cytoplasmic domain of at least 350 kDa. Mol. Biol. Cell *4*, 679–696.

Lippincott-Schwartz, J. (1993). Bidirectional membrane traffic between the endoplasmic reticulum and the Golgi apparatus. Trends Cell Biol. *3*, 81–88.

Lippincott-Schwartz, J., Cole, N.B., Marotta, A., Conrad, P.A., and Bloom, G.S. (1995). Kinesin is the motor for microtubule-mediated Golgi-to-ER membrane traffic. J. Cell Biol. *128*, 293–306.

Lippincott-Schwartz, J., Donaldson, J.G., Schweizer, A., Berger, E.G., Hauri, H.-P., Yuan, L.C., and Klausner, R.D. (1990). Microtubule-dependent retrograde transport of proteins into the ER in the presence of Brefeldin A suggests an ER recycling pathway. Cell *60*, 821–836.

Lippincott-Schwartz, J., Yuan, L.C., Bonifacino, J.S., and Klausner, R.D. (1989). Rapid redistribution of Golgi proteins into the ER in cells treated with brefeldin A: evidence for membrane cycling from the Golgi to the ER. Cell *56*, 801–813.

Lippincott-Schwartz, J., Yuan, L., Tipper, C., Amherdt, M., Orci, L., and Klausner, R.D. (1991). Brefeldin A's effects on endosomes, lysosomes and the TGN suggest a general mechanism for regulating organelle structure and membrane traffic. Cell *67*, 601–616.

Lombillo, V.A., Nislow, C., Yen, T.J., Gelfand, V.I., and McIntosh, J.R. (1995). Antibodies to the kinesin motor domain and CENP-E inhibit microtubule depolymerization-dependent motion of chromosomes in vitro. J.Cell Biol. *128*, 107–115.

Lucocq, J.M., and Warren, G. (1987). Fragmentation and partitioning of the Golgi apparatus during mitosis in HeLa cells. EMBO J. *11*, 3239–3246.

Luzio, J., Brake, B., Banting, G., Howell, K., Braghetta, P., and Stanley, K. (1990). Identification, sequencing and expression of an integral membrane protein of the trans-Golgi network (TGN38). Biochem. J. *270*, 97–102.

Murray, A. (1991). Cell cycle extracts. Methods Cell Biol. *36*, 581–605.

Nakamura, N., Rabouille, C., Watson, R., Nilsson, T., Hui, N., Slusarewicz, P., Kreis, T.E., and Warren, G. (1995). Characterization of a *cis*-Golgi matrix protein, GM130. J. Cell Biol. *131*, 1715–1726.

Nakata, T., and Hirokawa, N. (1995). Point mutation of adenosine triphosphate-binding motif generated rigor kinesin that selectively blocks anterograde lysosome membrane transport. J. Cell Biol. *131*, 1039–1053.

Niclas, J., Allan, V.J., and Vale, R.D. (1996). Cell cycle regulation of dynein association with membranes modulates microtubule-based organelle transport. J. Cell Biol. *133*, 585–593.

Niclas, J., Navone, F., Hom Booher, N., and Vale, R.D. (1994). Cloning and localization of a conventional kinesin motor expressed exclusively in neurons. Neuron *12*, 1059–1072.

Orci, L., Tagaya, M., Amherdt, M., Perrelet, A., Donaldson, J.G., Lippincott-Schwartz, J., Klausner, R.D., and Rothman, J.E. (1991). Brefeldin A, a drug that blocks secretion, prevents the assembly of non-clathrin-coated buds on Golgi cisternae. Cell *64*, 1183–1195.

Pepperkok, R., Scheel, J., Horstmann, H., Hauri, H.P., Griffiths, G., and Kreis, T.E. (1993). Beta-COP is essential for biosynthetic membrane transport from the endoplasmic reticulum to the Golgi complex in vivo. Cell *74*, 71–82.

Pfister, K.K., Wagner, M.C., Stenoien, D.L., Brady, S.T., and Bloom, G.S. (1989). Monoclonal antibodies to kinesin heavy and light chains stain vesicle-like structures, but not microtubules, in cultured cells. J. Cell Biol. *108*, 1453–1464.

Presley, J.F., Cole, N.B., Schroer, T.A., Hirschberg, K., Zaal, K.J.M., and Lippincott-Schwartz, J. (1997). ER-to-Golgi transport visualized in living cells. Nature *389*, 81–85.

Reaves, B., and Banting, G. (1992). Peturbation of the morphology of the *trans*-Golgi network following brefeldin A treatment: redistribution of a TGN-specific integral membrane protein, TGN38. J. Cell Biol. *116*, 85–94.

Robbins, E., and Gonatas, N.K. (1964). The ultrastructure of a mammalian cell during the mitotic cycle. J. Cell Biol. *21*, 429–463.

Robertson, A., and Allan, V. (1997). Cell cycle regulation of organelle transport. In: Progress in Cell Cycle Research, ed. L. Meijer, S. Guidet, and M. Philippe, New York: Plenum Press, 59–75.

Rodionov, V., Gyoeva, F., and Gelfand, V. (1991). Kinesin is responsible for centrifugal movement of pigment granules in melanophores. Proc. Natl. Acad. Sci. USA *88*, 4956–4960.

Rogalski, A.A., and Singer, S.J. (1984). Associations of elements of the Golgi apparatus with microtubules. J. Cell Biol. *99*, 1092–1100.

Sawin, K.E., Mitchison, T.J., and Wordeman, L.G. (1992). Evidence for kinesin-related proteins in the mitotic apparatus using peptide antibodies. J.Cell Sci. *101*, 303–313.

Sciaky, N., Presley, J., Smith, C., Zaal, K.J.M., Cole, N., Moreira, J.E., Terasaki, M., Siggia, E., and Lippincott-Schwartz, J. (1997). Golgi tubule traffic and the effects of brefeldin A visualized in living cells. J. Cell Biol. *139*, 1137–1155.

Shima, D., Hladar, K., Pepperkok, R., Watson, R., and Warren, G. (1997). Partitioning of the Golgi apparatus during mitosis in living HeLa cells. J. Cell Biol. *137*, 1211–1228.

Shima, D.T., Cabrera-Poch, N., Pepperkok, R., and Warren, G. (1998). An ordered inheritance strategy for the Golgi apparatus: visualization of mitotic disassembly reveals a role for the mitotic spindle. J. Cell Biol. *141*, 955–966.

Tanaka, Y., Kanai, Y., Okada, Y., Nonaka, S., Takeda, S., Harada, A., and Hirokawa, N. (1998). Targeted disruption of mouse conventional kinesin heavy chain, kif5B, results in abnormal perinuclear clustering of mitochondria. Cell *93*, 1147–1158.

Tuma, M.C., Zill, A., Le Bot, N., Vernos, I., and Gelfand, V. (1998). Heterotrimeric kinesin II is the microtubule motor protein responsible for pigment dispersion in *Xenopus* melanophores. J. Cell Biol. *143*, 1547–1558.

Vale, R.D., and Hotani, H. (1988). Formation of membrane networks in vitro by kinesin-driven microtubule movement. J. Cell Biol. *107*, 2233–2242.

Vale, R.D., and Toyoshima, Y.Y. (1988). Rotation and translocation of microtubules in vitro induced by dyneins from *Tetrahymena* cilia. Cell *52*, 459–469.

Vaux, D., Tooze, J., and Fuller, S. (1990). Identification by anti-idiotype antibodies of an intracellular membrane protein that recognizes a mammalian endoplasmic reticulum retention signal. Nature *345*, 495–502.

Warren, G. (1985). Membrane traffic and organelle division. Trends Biochem. Sci. *10*, 439–443.

Waterman-Storer, C.M., Gregory, J., Parsons, S.F., and Salmon, E.D. (1995). Membrane/microtubule tip attachment complexes (TACs) allow the assembly dynamics of plus ends to push and pull membranes into tubulovesicular networks in interphase *Xenopus* egg extracts. J. Cell Biol. *130*, 1161–1169.

Wessel, D., and Flugge, U.I. (1984). A method for the quantitative recovery of protein in dilute solution in the presence of detergents and lipids. Anal. Biochem. *138*, 141–143.

Wood, S.A., Park, J.E., and Brown, W.J. (1991). Brefeldin A causes a microtubule-mediated fusion of the trans-Golgi network and early endosomes. Cell *67*, 591–600.

Wright, B.W., Terasaki, M., and Scholey, J.M. (1993). Roles of kinesin and kinesin-like proteins in sea urchin embryonic cell division: evaluation using antibody microinjection. J. Cell Biol. *123*, 681–689.

Wubbolts, R., Fernandez-Borja, M., Jordens, I., Reits, E., Dusseljee, S., Echeverris, C., Vallee, R., and Neefjex, J. (1999). Opposing motor activities of dynein and kinesin determine retention and transport of MHC class II-containing compartments. J. Cell Sci. *112*, 785–795.

Yang, Z., and Goldstein, L.S.B. (1998). Characterization of the KIF3C neural kinesin-like motor from mouse. Mol. Biol. Cell *9*, 249–261.